Physics Letters B 696 (2011) 473–477

Contents lists available at ScienceDirect

Physics Letters B

www.elsevier.com/locate/physletb

Exclusive processes in electron–ion collisions

E.R. Cazaroto [a], F. Carvalho [b], V.P. Gonçalves [c], M.S. Kugeratski [d], F.S. Navarra [a,*]

[a] Instituto de Física, Universidade de São Paulo, C.P. 66318, 05315-970 São Paulo, SP, Brazil
[b] Departamento de Ciências Exatas e da Terra, Universidade Federal de São Paulo, Campus Diadema, Rua Prof. Artur Riedel, 275, Jd. Eldorado, 09972-270 Diadema, SP, Brazil
[c] Instituto de Física e Matemática, Universidade Federal de Pelotas, Caixa Postal 354, 96010-900 Pelotas, RS, Brazil
[d] Centro de Engenharia da Mobilidade, Universidade Federal de Santa Catarina, Campus Universitário, Bairro Bom Retiro 89219-905, Joinville, SC, Brazil

ARTICLE INFO

Article history:
Received 14 September 2010
Received in revised form 30 December 2010
Accepted 31 December 2010
Available online 14 January 2011
Editor: J.-P. Blaizot

Keywords:
High energy physics
Quantum chromodynamics
Deep inelastic scattering
Electron ion collisions
Parton saturation

ABSTRACT

The exclusive processes in electron–ion (eA) interactions are an important tool to investigate the QCD dynamics at high energies as they are in general driven by the gluon content of the target which is strongly subject to parton saturation effects. In this Letter we compute the cross sections for the exclusive vector meson production as well as the deeply virtual Compton scattering (DVCS) relying on the color dipole approach and considering the numerical solution of the Balitsky–Kovchegov equation including running coupling corrections (rcBK). The production cross sections obtained with the rcBK solution and bCGC parametrization are very similar, the former being slightly larger.

Exclusive processes in deep inelastic scattering (DIS) have appeared as key reactions to trigger the generic mechanism of diffractive scattering (for a recent review see, e.g. [1]). In particular, diffractive vector meson production and Deeply Virtual Compton Scattering (DVCS) have been extensively studied at HERA and provide a valuable probe of the QCD dynamics at high energies. The usual Compton scattering is the process $\gamma + e \to \gamma + e$, where γ is a real photon and e is an electron. In the Deep Inelastic Scattering (DIS) regime an electron emits a virtual photon (γ^*) that interacts with the target, which can be, e.g., a nucleus A. If in the final state we have a real photon ($\gamma^* + A \to \gamma + Y$) we call this process Deeply Virtual Compton Scattering. The processes mentioned above are driven by the gluon content of the target (proton or nucleus) which is strongly subject to parton saturation effects as well as to nuclear shadowing corrections when one considers scattering on nuclei (see e.g. [2]). In particular, the cross sections for exclusive processes in DIS are proportional to the square of the scattering amplitude, which makes them strongly sensitive to the underlying QCD dynamics. In a recent paper [3] we have estimated the coherent and incoherent cross sections for exclusive ρ and J/Ψ production considering the color dipole approach and phenomenological saturation models which describe the scarce F_2^A data as well as the HERA data. Our results demonstrated that the coherent production of vector mesons is dominant, with a small contribution coming from incoherent processes. Moreover, our results indicate that the experimental study of these processes is feasible in future electron–ion collider, as e.g. the eRHIC [4] or LHeC [5]. In this Letter we complement our previous analysis including ϕ production and extending our study to the nuclear DVCS (see also [6]). Moreover, we review our results for ρ and J/Ψ production making use of the numerical solution of the Balitsky–Kovchegov equation [7,8] including running coupling corrections [9–11] in order to estimate the contribution of the saturation physics to exclusive processes. Our main motivation is associated to the fact that the improved BK equation has been shown to be really successful when applied to the description of the ep HERA data on inclusive and diffractive proton structure function [12–14], as well as on exclusive processes [15] and on the forward hadron spectra in pp and dA collisions [14,16].

Let us start presenting a brief review of exclusive processes in electron–ion collisions (for details see [3,17]). In the color dipole approach the exclusive production $\gamma^* A \to EY$ ($E = \rho, \phi, J/\Psi$ or γ) in electron–nucleus interactions at high energies can be factorized in terms of the fluctuation of the virtual photon into a $q\bar{q}$ color dipole, the dipole–nucleus scattering by a color singlet exchange and the recombination into the exclusive final state E. This process is characterized by a rapidity gap in the final state. If the nucleus scatters elastically, $Y = A$, the process is called coherent

* Corresponding author.
E-mail address: navarra@if.usp.br (F.S. Navarra).

0370-2693
doi:10.1016/j.physletb.2010.12.071

production and the corresponding integrated cross section is given in the high energy regime (large coherence length: $l_c \gg R_A$) by [3,17]

$$\sigma^{coh}\big(\gamma^* A \to EA\big) = \int d^2\boldsymbol{b}\left|\mathcal{N}^A(x,\boldsymbol{r},\boldsymbol{b})\right|^2 \tag{1}$$

where

$$\langle\mathcal{N}\rangle = \int d^2\boldsymbol{r}\int dz\,\Psi_E^*(\boldsymbol{r},z)\mathcal{N}^A(x,\boldsymbol{r},\boldsymbol{b})\Psi_{\gamma^*}\big(\boldsymbol{r},z,Q^2\big) \tag{2}$$

and $\mathcal{N}(x,\boldsymbol{r},\boldsymbol{b})$ is the forward dipole-target scattering amplitude for a dipole with size $\boldsymbol{r}$ and impact parameter $\boldsymbol{b}$ which encodes all the information about the hadronic scattering, and thus about the non-linear and quantum effects in the hadron wave function. On the other hand, if the nucleus scatters inelastically, i.e. breaks up ($Y = X$), the process is denoted incoherent production. In this case one sums over all final states of the target nucleus, except those that contain particle production. The t slope is the same as in the case of a nucleon target. Therefore we have:

$$\sigma^{inc}\big(\gamma^* A \to EX\big) = \frac{|\mathcal{I}m\mathcal{A}(s,t=0)|^2}{16\pi B_E} \tag{3}$$

where at high energies ($l_c \gg R_A$) [17]:

$$|\mathcal{I}m\mathcal{A}|^2 = \int d^2\boldsymbol{b}\,T_A(\boldsymbol{b})\left\langle\sigma_{dp}\exp\left[-\frac{1}{2}\sigma_{dp}T_A(\boldsymbol{b})\right]\right\rangle^2 \tag{4}$$

and σ_{dp} is the dipole–proton cross section, which in the eikonal approximation it is given by:

$$\sigma_{dp}(x,\boldsymbol{r}) = 2\int d^2\boldsymbol{b}\,\mathcal{N}^p(x,\boldsymbol{r},\boldsymbol{b}). \tag{5}$$

In the incoherent case, the $q\bar{q}$ pair attenuates with a constant absorption cross section, as in the Glauber model, except that the whole exponential is averaged rather than just the cross section in the exponent. As discussed in [3], the coherent and incoherent cross sections depend differently on t. At small-t ($-tR_A^2/3 \ll 1$) coherent production dominates, with the signature being a sharp forward diffraction peak. On the other hand, incoherent production will dominate at large-t ($-tR_A^2/3 \gg 1$), with the t-dependence being to a good accuracy the same as in the production off free nucleons.

In Eqs. (2) and (4) the functions $\Psi^\gamma(z,\boldsymbol{r})$ and $\Psi^E(z,\boldsymbol{r})$ are the light-cone wavefunctions of the photon and the exclusive final state, respectively. The variable $\boldsymbol{r}$ defines the relative transverse separation of the pair (dipole) and z ($1-z$) is the longitudinal momentum fraction of the quark (antiquark). In the dipole formalism, the light-cone wavefunctions $\Psi(z,\boldsymbol{r})$ in the mixed representation (r,z) are obtained through a two-dimensional Fourier transform of the momentum space light-cone wavefunctions $\Psi(z,\boldsymbol{k})$. The photon wavefunctions are well known in literature [18]. For the meson wavefunction, we have considered the Gauss-LC model of Ref. [18]. The motivation for this choice is its simplicity and the fact that the results are not very sensitive to differences between the models analyzed in [18]. We choose the quark masses to be $m_{u,d,s} = 0.14$ GeV and $m_c = 1.4$ GeV. The parameters for the meson wavefunction can be found in Ref. [18]. In the DVCS case, as one has a real photon at the final state, only the transversely polarized overlap function contributes to the cross section. Summed over the quark helicities, for a given quark flavor f it is given by [19],

$$\big(\Psi_\gamma^*\Psi\big)_T^f = \frac{N_c\alpha_{\rm em}e_f^2}{2\pi^2}\big\{\big[z^2+\bar{z}^2\big]\varepsilon_1K_1(\varepsilon_1 r)\varepsilon_2K_1(\varepsilon_2 r) + m_f^2K_0(\varepsilon_1 r)K_0(\varepsilon_2 r)\big\}, \tag{6}$$

where we have defined the quantities $\varepsilon_{1,2}^2 = z\bar{z}Q_{1,2}^2 + m_f^2$ and $\bar{z} = (1-z)$. Accordingly, the photon virtualities are $Q_1^2 = Q^2$ (incoming virtual photon) and $Q_2^2 = 0$ (outgoing real photon).

In order to estimate the coherent production in eA collisions we need to specify the forward dipole–nucleus scattering amplitude, $\mathcal{N}^A(x,\boldsymbol{r},\boldsymbol{b})$. Following [3] we will use in our calculations the model proposed in Ref. [20], which describes the current experimental data on the nuclear structure function as well as includes the impact parameter dependence in the dipole nucleus cross section. In this model the forward dipole–nucleus amplitude is given by

$$\mathcal{N}^A(x,\boldsymbol{r},\boldsymbol{b}) = 1-\exp\left[-\frac{1}{2}\sigma_{dp}\big(x,\boldsymbol{r}^2\big)T_A(\boldsymbol{b})\right], \tag{7}$$

where σ_{dp} is the dipole–proton cross section and $T_A(\boldsymbol{b})$ is the nuclear profile function, which is obtained from a 3-parameter Fermi distribution for the nuclear density normalized to A. The above equation sums up all the multiple elastic rescattering diagrams of the $q\bar{q}$ pair and is justified for large coherence length, where the transverse separation $\boldsymbol{r}$ of partons in the multiparton Fock state of the photon becomes a conserved quantity, i.e. the size of the pair $\boldsymbol{r}$ becomes eigenvalue of the scattering matrix.

In our approach the coherent [Eq. (1)] and incoherent [Eq. (3)] cross sections can be calculated in terms of the dipole–proton cross section or the forward dipole–proton scattering amplitude [ee Eq. (5)], which is a solution of the BK equation. As the leading order solution of the BK equation was not able to describe the HERA data, in Ref. [3] we have used the GBW [21] and bCGC [18] parametrizations for $\mathcal{N}^p$ as input in our calculations. However, in the last years the next-to-leading order corrections to the BK equation were calculated [9–11]. Such calculation allows one to estimate the soft gluon emission and running coupling corrections to the evolution kernel. The authors have verified that the dominant contributions come from the running coupling corrections, which allow us to determine the scale of the running coupling in the kernel. The solution of the improved BK equation was studied in detail in Refs. [10,22]. Basically, one finds that the running of the coupling reduces the speed of the evolution to values compatible with experimental data. In [12] a global analysis of the small x data for the proton structure function using the improved BK equation was performed (see also Ref. [13]). In contrast to the BK equation at leading logarithmic $\alpha_s\ln(1/x)$ approximation, which fails to describe the HERA data, the inclusion of running coupling effects in the evolution renders the BK equation compatible with them (see also [14–16]). It is important to emphasize that the impact parameter dependence was not taken into account in Ref. [12], the normalization of the dipole cross section was fitted to data and two distinct initial conditions, inspired by the Golec-Biernat–Wüsthoff (GBW) [21] and McLerran–Venugopalan (MV) [23] models, were considered. The predictions resulted to be almost independent of the initial conditions and, besides, it was observed that it is impossible to describe the experimental data using only the linear limit of the BK equation. The parametrizations obtained in [12] were very successful in reproducing DIS data but it remains to seen whether they can also be used to describe data from RHIC. Other parametrizations of dipole cross sections had to be slightly modified in order to account for RHIC data [24].

In what follows we calculate the exclusive observables using as input in our calculations the solution of the running coupling Balitsky–Kovchegov (rcBK) evolution equation. We make use of the public-use code available in [25]. In numerical calculations we have considered the GBW initial condition for the evolution. Furthermore, we compare the rcBK predictions with those from the bCGC model used in our previous calculation [3]. Moreover,

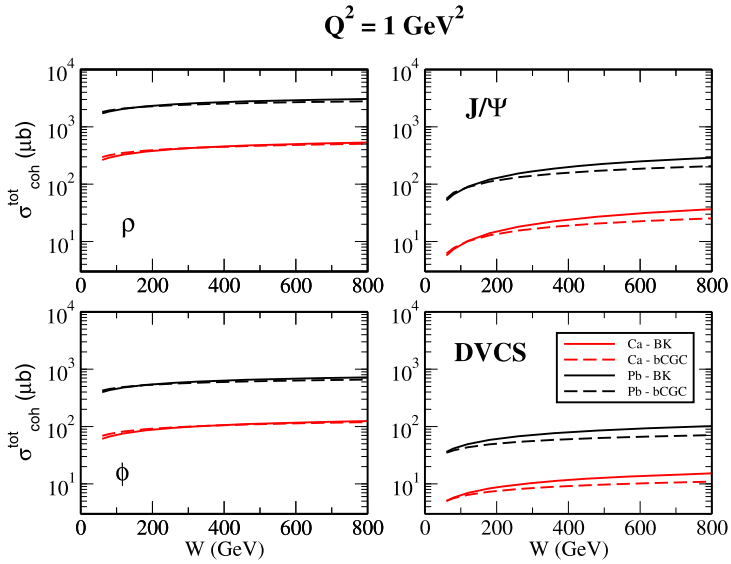

Fig. 1. (Color online.) Energy dependence of the coherent cross section at different final states and $Q^2 = 1$ GeV^2.

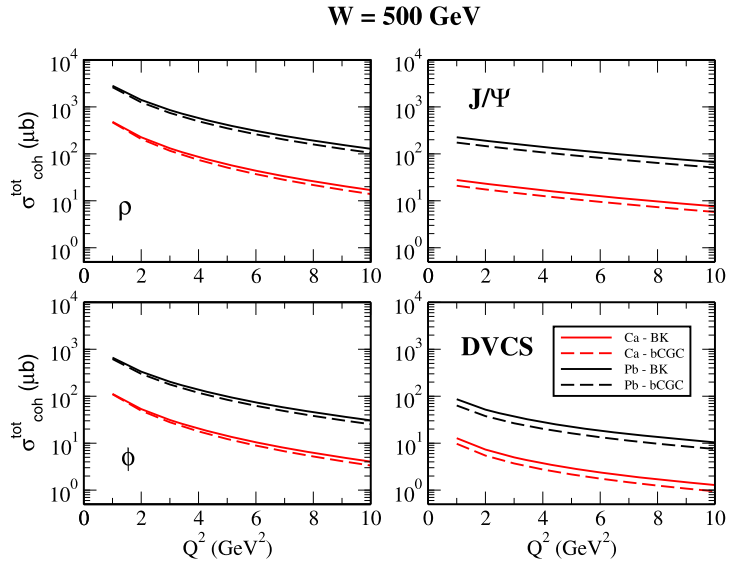

Fig. 2. (Color online.) Dependence on the photon virtuality of the coherent cross section for different final states and $W = 500$ GeV.

in order to calculate the incoherent cross section for vector meson production we will use the following parametrization of the diffractive slope

$$B_V(Q^2) = 0.60\left[\frac{14}{(Q^2 + M_V^2)^{0.26}} + 1\right] \tag{8}$$

obtained from a fit to experimental data referred in Ref. [26]. In the DVCS case we take the experimental parametrization [27], $B(Q^2) = a[1 - b\log(Q^2/Q_0^2)]$, with $a = 6.98 \pm 0.54$ GeV^2, $b = 0.12 \pm 0.03$ and $Q_0^2 = 2$ GeV^2.

In Fig. 1 we show the coherent production cross section as a function of the photon-target c.m.s energy, W, for a fixed photon virtuality $Q^2 = 1$ GeV^2. Each one of the panels shows the results obtained for one specific final state. In each single figure the two upper (lower) curves show the results for a Pb (Ca) target. In all figures the dashed (solid) lines are obtained with the bCGC (rcBK) dipole cross section. Fig. 2 shows the same cross sections, this time as a function of Q^2 for a fixed energy, $W = 500$ GeV. Figs. 3 and 4 are the exact analogues (of Figs. 1 and 2) for the corresponding incoherent cross sections.

The curves in the figures have the merit of being the first concrete predictions made for these processes with the help of the recently obtained rcBK dipole cross section. They present some features which are expected and some other features which could not have been anticipated without a quantitative calculation. In first place we observe, as it should be, that all cross sections grow with W and fall with Q^2. The first feature is related solely to the nature of the dipole cross section, which grows with the energy, whereas the second feature comes from the dipole wave functions. We can also see from the figures that, at least for the two cases considered (bCGC and rcBK), the production cross sections are not very strongly dependent on the choice of the dipole cross section.

At low Q^2 and low W the bCGC and rcBK production cross sections are indistinguishable one from the other because the dipole cross sections tend to coincide. These latter have been tuned to fit DIS data, which are taken in this kinematical region. Another expected feature is the observed decrease of the cross sections with

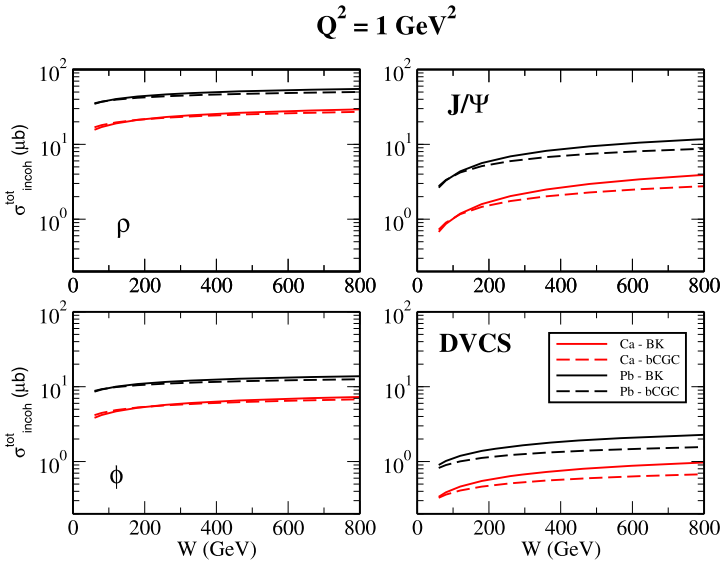

Fig. 3. (Color online.) Energy dependence of the incoherent cross section for different final states and $Q^2 = 1$ GeV^2.

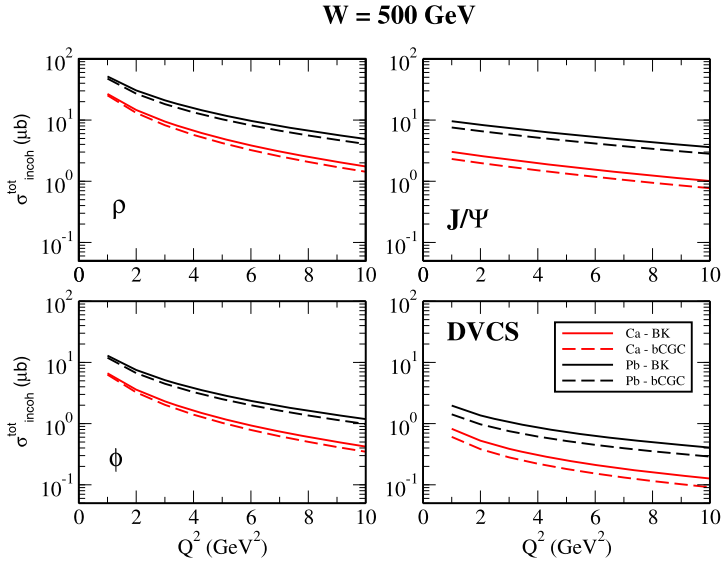

Fig. 4. (Color online.) Dependence on the photon virtuality of the incoherent cross section for different final states and $W = 500$ GeV.

increasing vector meson masses, which comes from the wave functions.

Differences are expected to appear at higher energies, where we enter the lower x (extrapolation) region. In all cases we see that the results obtained with the rcBK cross section are larger than those obtained with the bCGC one. This is related to the fact that the numerical solutions of the BK equation tend to reach later the unitarity limit [28]. In the first estimates, with a fixed coupling, the solutions of the BK equation would saturate too fast. In subsequent studies it was found that running coupling corrections to the BK kernel could bring the evolution speed down to values compatible with those extracted from data, but still larger than those found in other parametrizations, such as the bCGC one. Due to this fact, the results obtained with the rcBK dipole cross section grow faster with energy than those obtained with the bCGC one.

A curious feature in the figures is that *the differences between bCGC and rcBK are larger for heavier vector mesons*. This can be understood looking carefully at the integrand of (1), which is the product of the wave functions, containing information about the masses, and the dipole cross section. As a function of the dipole size r the difference between bCGC and rcBK is mostly in the low to intermediate r region, where the bCGC is always below the rcBK dipole cross section. At large r the two cross sections are close to each other. The overlap function, i.e., $(\Psi_\gamma^* \Psi)^f$ given by (6) (with the inclusion of the longitudinally polarized overlap function), has peaks at different locations. The ρ is a larger state and its overlap function peaks at much larger values than the J/ψ overlap function. In this way it gives a stronger weight to larger r where the differences between bCGC and rcBK are smaller. The same thing happens to the ϕ. On the other hand, the J/ψ overlap function peaks at smaller r where the dipole cross sections are more different from each other. A similar behavior is verified in the DVCS case.

As shown in [28], at increasing values of the energy W (and thus of smaller of x) the difference between rcBK and bCGC moves to smaller values of r, a region which is suppressed by the overlap

functions of the ρ and ϕ. This explains why the ρ (and also the ϕ) production cross sections are almost the same for rcBK and bCGC dipole cross sections for all the energies considered, as it can be seen on the right side of Figs. 1 and 3.

In Figs. 2 and 4 we would expect to see a convergence of the curves for higher values of Q^2. In this region the dipoles are small and all cross sections should approach the color transparency regime. In fact, a difference between them persists even at large Q^2 because in the expressions used here there is no DGLAP evolution, which would bring the dipole cross sections together.

As a summary, we presented a systematic analysis of exclusive production in small-x deep inelastic electron–ion scattering in terms of the non-linear QCD dynamics. This was the first calculation (of these observables) using the solution of the BK equation improved with running coupling corrections. In this work we obtain predictions for the exclusive production of vector mesons and DVCS. Our analysis confirms the dominance of the coherent production with a small contribution coming from incoherent processes, a result previously found in [3]. Our main result is that the BK evolution equation implies larger cross sections for exclusive processes than the phenomenological model proposed in [18], the so-called bCGC model. Our predictions for both vector meson and DVCS production are relevant for the physics programs of the future experiments eRHIC and LHeC.

Acknowledgements

This work was partially financed by the Brazilian funding agencies CNPq and FAPESP.

References

[1] L. Schoeffel, Prog. Part. Nucl. Phys. 65 (2010) 9.
[2] B.Z. Kopeliovich, I. Schmidt, M. Siddikov, Phys. Rev. D 81 (2010) 094013; B.Z. Kopeliovich, I. Schmidt, M. Siddikov, Phys. Rev. D 82 (2010) 014017.
[3] V.P. Goncalves, M.S. Kugeratski, M.V.T. Machado, F.S. Navarra, Phys. Rev. C 80 (2009) 025202.
[4] A. Deshpande, R. Milner, R. Venugopalan, W. Vogelsang, Ann. Rev. Nucl. Part. Sci. 55 (2005) 165.
[5] J.B. Dainton, M. Klein, P. Newman, E. Perez, F. Willeke, JINST 1 (2006) P10001.
[6] M.V.T. Machado, Eur. Phys. J. C 59 (2009) 769.
[7] I.I. Balitsky, Phys. Rev. Lett. 81 (1998) 2024; I.I. Balitsky, Phys. Lett. B 518 (2001) 235; I.I. Balitsky, A.V. Belitsky, Nucl. Phys. B 629 (2002) 290.
[8] Y.V. Kovchegov, Phys. Rev. D 60 (1999) 034008; Y.V. Kovchegov, Phys. Rev. D 61 (2000) 074018.
[9] Y.V. Kovchegov, H. Weigert, Nucl. Phys. A 784 (2007) 188; Y.V. Kovchegov, H. Weigert, Nucl. Phys. A 789 (2007) 260; Y.V. Kovchegov, J. Kuokkanen, K. Rummukainen, H. Weigert, Nucl. Phys. A 823 (2009) 47.
[10] J.L. Albacete, Y.V. Kovchegov, Phys. Rev. D 75 (2007) 125021.
[11] I. Balitsky, Phys. Rev. D 75 (2007) 014001; I. Balitsky, G.A. Chirilli, Phys. Rev. D 77 (2008) 014019.
[12] J.L. Albacete, N. Armesto, J.G. Milhano, C.A. Salgado, Phys. Rev. D 80 (2009) 034031.
[13] H. Weigert, J. Kuokkanen, K. Rummukainen, AIP Conf. Proc. 1105 (2009) 394.
[14] M.A. Betemps, V.P. Goncalves, J.T. de Santana Amaral, Eur. Phys. J. C 66 (2010) 137.
[15] V.P. Goncalves, M.V.T. Machado, A.R. Meneses, Eur. Phys. J. C 68 (2010) 133.
[16] J.L. Albacete, C. Marquet, Phys. Lett. B 687 (2010) 174.
[17] B.Z. Kopeliovich, J. Nemchik, A. Schafer, A.V. Tarasov, Phys. Rev. C 65 (2002) 035201.
[18] H. Kowalski, L. Motyka, G. Watt, Phys. Rev. D 74 (2006) 074016.
[19] M. Wusthoff, A.D. Martin, J. Phys. G 25 (1999) R309.
[20] N. Armesto, Eur. Phys. J. C 26 (2002) 35.
[21] K. Golec-Biernat, M. Wüsthoff, Phys. Rev. D 59 (1999) 014017; K. Golec-Biernat, M. Wüsthoff, Phys. Rev. D 60 (1999) 114023.
[22] J.L. Albacete, Phys. Rev. Lett. 99 (2007) 262301.
[23] L. McLerran, R. Venugopalan, Phys. Rev. D 49 (1994) 2233.
[24] V.P. Goncalves, M.S. Kugeratski, M.V.T. Machado, F.S. Navarra, Phys. Lett. B 643 (2006) 273.
[25] http://www-fp.usc.es/phenom/rcbk.
[26] A.C. Caldwell, M.S. Soares, Nucl. Phys. A 696 (2001) 125.
[27] F.D. Aaron, et al., H1 Collaboration, Phys. Lett. B 659 (2008) 796.
[28] A systematic comparison of the energy behavior of different dipole amplitudes (including the rcBK one) can be found in: M.A. Betemps, V.P. Goncalves, J.T. de Santana Amaral, Eur. Phys. J. C 66 (2010) 137.